

Hydrogen-Bond Patterns in Liquid Water¹

A. Rahman^{1b} and F. H. Stillinger*^{1c}

Contribution from the Argonne National Laboratory, Argonne, Illinois 60439, and Bell Laboratories, Murray Hill, New Jersey 07974. Received July 11, 1973

Abstract: Distributions of non-short-circuited hydrogen-bond polygons in water have been constructed, using configurations generated by a molecular dynamics simulation for the liquid. The thermodynamic state analyzed has temperature 10° and mass density 1 g/cm³. The distributions are broad and show nontrivial contributions from polygons with sizes greater than eight. The results seem to be inconsistent with the view of liquid water as a recognizably disrupted version of any known ice or hydrate crystal structure.

The capacity to form intermolecular hydrogen bonds is the single most important molecular feature underlying the properties of liquid and solid water. These bonds affect both macroscopic thermodynamic behavior as well as microscopic structure. They are furthermore decisive in explaining kinetic properties.

It is natural then that past "models" for liquid water and aqueous solutions should have forms strongly influenced by the demands of hydrogen bonding.^{2a} In

(1) (a) Part of the work carried out at the Argonne National Laboratory was supported by the U. S. Atomic Energy Commission; (b) Argonne National Laboratory; (c) Bell Laboratories.

(2) (a) J. L. Kavenau, "Water and Solute-Water Interactions,"

particular, there has been a tendency to rely on known ice or hydrate crystal structures to suggest which class of hydrogen-bond patterns might dominate in the liquid. Thus we have seen advocated for the liquid at various times a self-clathrate model,^{2b} a distended ice Ih with interstitials,³ ice-like "clusters" suspended in unbonded water,⁴ or small aggregates bonded in the

Holden-Day, San Francisco, Calif., 1964. (b) L. Pauling, "Hydrogen Bonding," D. Hadzi and H. W. Thompson, Ed., Pergamon Press, London, 1959, pp 1-5.

(3) M. D. Danford and H. A. Levy, *J. Amer. Chem. Soc.*, **84**, 3965 (1962).

(4) H. S. Frank and W.-Y. Wen, *Discuss. Faraday Soc.*, **24**, 133 (1957).

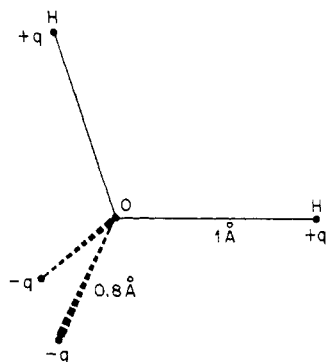


Figure 1. Four-point-charge model used to define the ST2 pair interaction. All angles at the oxygen position (O) are equal to the ideal tetrahedral angle $109^\circ 28'$.

pattern of ice II.⁵ To these might peripherally be added the statistically well-defined lattice^{6,7} and cell⁸ theories for liquid water that have appeared recently, based structurally upon the body-centered cubic crystal of ice VII.⁹

Upon melting crystalline water to form the liquid, the restraint of spatial periodicity for molecular positions disappears. It therefore seems plausible that a far richer set of hydrogen-bonded structures should be available in the liquid than that suggested by crystal structures alone. It is possible that "simple" models of the type mentioned above may be valuable in explaining thermodynamic behavior of the pure liquid and its solutions. However, a conceptually less restrictive technique should be available to judge the extent to which local structures implicit in these models are realistic.

It has recently become feasible^{10,11} to simulate liquid water at the molecular level using rapid digital computers, on account of accumulating knowledge about water molecule interactions. Our purpose in this paper is to use the data generated by a molecular dynamics simulation of water to characterize the spatial patterns of hydrogen bonds in the liquid.

Potential of Interaction

The essence of the molecular dynamics technique is that the digital computer solves coupled equations of classical motion for a selected set of molecules (216 in the case to be considered here) subject to a precisely specified potential of interaction. Boundary conditions are selected to fix the density,¹² and initial conditions implicitly determine the temperature. The temporal evolution of the dynamical system generates a set of molecular configurations, about which diverse structural (and kinetic) queries can be posed.

The total potential energy used in the present simulation consists of a sum of effective pair potentials.^{13,14}

- (5) S. R. Erlander, *J. Macromol. Sci., Chem.*, **2**, 595 (1968).
- (6) G. M. Bell, *J. Phys. C*, **5**, 889 (1972).
- (7) (a) J. H. Gibbs and P. D. Fleming, submitted for publication; (b) D. E. O'Reilly, *Phys. Rev. A*, **7**, 1659 (1973).
- (8) O. Weres and S. A. Rice, *J. Amer. Chem. Soc.*, **94**, 8983 (1972).
- (9) C. Weir, S. Block, and G. Piermarini, *J. Res. Nat. Bur. Stand., Sect. C*, **69**, 275 (1965).
- (10) A. Rahman and F. H. Stillinger, *J. Chem. Phys.*, **55**, 3336 (1971).
- (11) F. H. Stillinger and A. Rahman, *J. Chem. Phys.*, **57**, 1281 (1972).
- (12) It has become traditional to employ periodic boundary conditions with a cubic unit cell, to eliminate spurious wall effects.
- (13) F. H. Stillinger, *J. Phys. Chem.*, **74**, 3677 (1970).
- (14) F. H. Stillinger, *J. Chem. Phys.*, **57**, 1780 (1972).

The effective pair potential (the present version¹⁵ is designated ST2 and differs slightly from that in ref 10 and 11) utilizes a rigid four-point-charge model for each water molecule, as shown in Figure 1. Specifically

$$V(1,2) = V_{LJ}(r_{12}) + S(r_{12})V_{el}(1,2) \quad (1)$$

where r_{12} is the separation between oxygen nuclei. The function V_{LJ} is a central interaction of the Lennard-Jones type

$$V_{LJ}(r) = 4\epsilon[(\sigma/r)^{12} - (\sigma/r)^6] \\ \epsilon = 5.2605 \times 10^{-16} \text{ erg} \quad (2) \\ \sigma = 3.10 \text{ \AA}$$

The four point charges $\pm q$ on each molecule contribute to 16 Coulombic interactions gathered in V_{el} . The charges have magnitudes

$$q = 0.2357e = 1.13194 \times 10^{-10} \text{ esu} \quad (3)$$

and are located at positions 1 (for positive charges) and 0.8 Å (negative charges) from the oxygen nucleus, so as to make angles $109^\circ 28'$ at that nucleus. Finally

$$S(r) = 0 \quad (0 \leq r \leq R_L) \\ = \frac{(r - R_L)^2(3R_U - R_L - 2r)}{(R_U - R_L)^3} \quad (4) \\ (R_L \leq r \leq R_U) \\ = 1 \quad (R_U \leq r)$$

with

$$R_L = 2.0160 \text{ \AA} \\ R_U = 3.1287 \text{ \AA} \quad (5)$$

The ST2 potential in conjunction with the molecular dynamics method appears to give a moderately good account of liquid water properties. Details will be published elsewhere.¹⁵ The important point to stress here is that the ST2 interaction is consistent with the strength and directionality of hydrogen bonds in real water, while at the same time its use for molecular dynamics entails no *a priori* prejudice toward specific hydrogen-bond patterns.

Hydrogen-Bond Definition

In accord with our previous usage^{10,11} we take the hydrogen bonds in an aggregate of water molecules to be purely configurational attributes. Specifically, we say that a pair i,j of molecules is hydrogen bonded if its potential $V(i,j)$ lies below some preassigned limit V_{HB} ; otherwise the pair is regarded as not hydrogen bonded. To be sure, arbitrariness is involved in the selection of V_{HB} . But it is important to note that a comfortable range will be available such that use of V_{HB} in this range for ordinary ice will cause the four crystallographic nearest neighbors to be hydrogen bonded to a given molecule, while none of the second neighbors will be considered so bonded.

The advantage of this sort of definition, for any choice of V_{HB} , is its precision. In any given arrangement of water molecules, the hydrogen bonds may unambiguously be identified. The spatial pattern of those

- (15) F. H. Stillinger and A. Rahman, *J. Chem. Phys.*, submitted for publication.

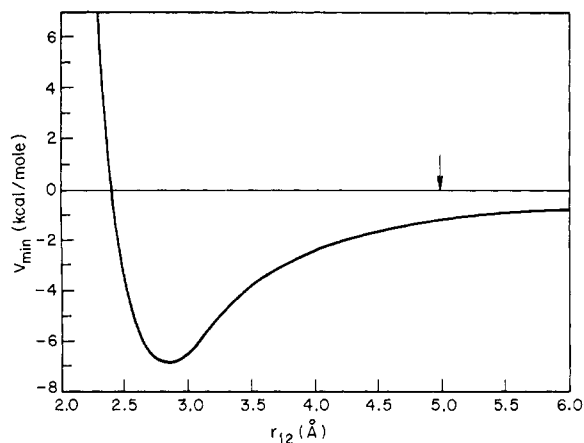


Figure 2. Plot of the minimum attainable interaction, with the ST2 effective pair potential, for variable separation r_{12} between the oxygen nuclei. The arrow (at 4.964 Å) marks the position beyond which molecular symmetry axes are precisely collinear.

hydrogen bonds then can be analyzed for characteristics of interest, such as connectivity, polygon closure, interlinking, concentrations of molecules with given numbers of hydrogen bonds, etc. For greatest insight, of course, one should exercise freedom to vary V_{HB} , to observe the resulting architectural implications for the hydrogen-bonded network.

The effective pair potential in eq 1 naturally depends on the relative orientation of the two molecules involved. At any fixed distance r_{12} between the oxygens, there will be one specific orientation (along with its symmetry-generated equivalents) which minimizes $V(1,2)$. The set of minimum values, denoted by V_{min} vs. r_{12} , has been plotted in Figure 2. The absolute minimum occurs at $r_{12} = 2.852$ Å, at which V_{min} is -6.839 kcal/mol, the negative of the maximum possible hydrogen-bond energy with the ST2 potential. In the neighborhood of this absolute minimum, the configuration involved has the "proton-donor" molecule pointing one of its OH bonds almost directly at the "proton-acceptor" oxygen. As r_{12} increases, though, the molecules rotate to bring their symmetry axes into closer alignment, and beyond the critical distance $r_{12} = 4.964$ Å these axes are precisely collinear. At all distances beyond $R_L = 2.016$ Å, the molecular planes are perpendicular in V_{min} configurations.

In ordinary hexagonal ice, second neighbors occur at about 4.5 Å. Chemical intuition therefore suggests that one ordinarily would want $V_{\text{HB}} < -1.7$ kcal/mol, considering the curve shown in Figure 2. Furthermore, it would be necessary with ST2 to require $V_{\text{HB}} > -4.5$ kcal/mol if all first neighbors in ice should be regarded as hydrogen bonded, since some of these neighbors are rotated away from the optimal interaction configuration.

Polygon Distributions

Our calculations have been devoted to enumeration of "non-short-circuited" polygons of hydrogen bonds. These are polygons with three or more sides no pair of whose vertices are linked by a hydrogen-bond path shorter (in number of bonds, not geometric length) than the minimal path within the polygon itself. Thus three molecules mutually bonded to form a triangle cannot be short-circuited, and that triangle will be

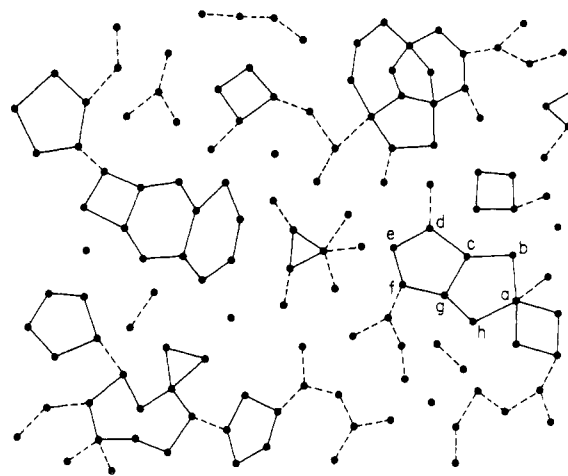


Figure 3. Schematic hydrogen-bond network. The non-short-circuited polygons have been identified with solid lines. For simplicity the structure of each molecule has been suppressed in favor of nondescript circles. Notice that some molecules may participate in no hydrogen bonds, while others can engage simultaneously in more than four. Polygon abcdefgh is short-circuited by bond cg and would not be counted, whereas polygons abcgh and cdefg would be counted.

counted. If two polygons share a single side, both *may* be counted (depending on other circumstances), but the larger encompassing polygon obtained by disregarding the common side would *not* be counted since it is short-circuited by that side. Figure 3 depicts in a schematic two-dimensional version the set of non-short-circuited polygons that would be identified in a random hydrogen-bonded network.

If one were motivated to select V_{HB} very small (but still negative), then the average number of "hydrogen bonds" per molecule would be very large, and many of these bonds would involve widely separated and weakly interacting pairs. The preponderance of non-short-circuited polygons would be triangles, though some larger sizes would always be present. In an infinite liquid water system, the average number of non-short-circuited polygons per molecule would diverge as V_{HB} approaches zero from below.

In the opposite extreme, where V_{HB} is permitted to approach the absolute minimum of the ST2 interaction, hydrogen bonds as defined in the present context would become very rare. The non-short-circuited polygons would likewise become rare. Furthermore their relative occurrence frequencies for different sizes would be affected, for the formation of a hydrogen bond with very low V_{HB} places stringent limits on the relative configuration of the pair involved. After V_{HB} moves below a certain threshold, triangles would be impossible since closure would twist molecules beyond mutually acceptable limits. Quadrilaterals, pentagons, hexagons, etc., in turn would become impossible, since pair configurations closer and closer to the absolute V_{min} are, when placed in sequence, more and more difficult to close in a given number of steps. Within the vanishing polygon population, therefore, the mean polygon size would diverge.

Neither of these mathematical limits illuminates the central issue in the present investigation, namely the local molecular order in water. Instead, the intermediate regime $-4.5 < V_{\text{HB}} < -1.7$ kcal/mol intro-

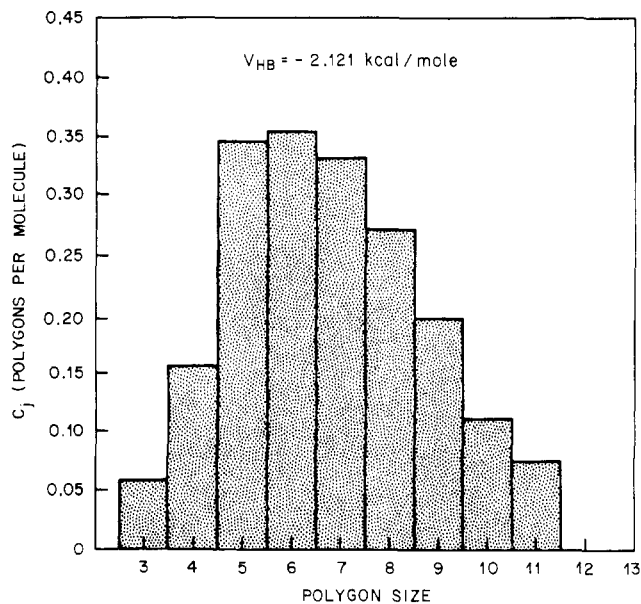


Figure 4. Non-short-circuited hydrogen-bond polygons, with $V_{\text{HB(I)}} = -2.121$ kcal/mol. The vertical axis gives the mean number of polygons per molecule in the entire liquid.

duced earlier is relevant. The conventional identification of hydrogen bonds in known aqueous crystal structures beside hexagonal ice surely falls within these rather wide limits, and it is interesting to note the sizes of the non-short-circuited polygons that occur in those structures. Table I collects the results. Significantly,

Table I. Sizes of Non-Short-Circuited Hydrogen-Bond Polygons in Various Aqueous Crystals

Crystal	Polygon sizes	Ref
Ice Ih	6	a
Ice Ic	6	a
Ice II	6	a
Ice III	5	a
Ice V	4	a
Ice VI	4, 8	a
Ices VII, VIII	6	a
Cl ₂ , Xe, CH ₄ , hydrates	5, 6	b
tert-Butylamine hydrate	4, 5, 6, 7	c

^a D. Eisenberg and W. Kauzmann, "The Structure and Properties of Water," Oxford University Press, New York, N. Y., 1969, Chapter 3. ^b L. Pauling, "The Nature of the Chemical Bond," Cornell University Press, Ithaca, N. Y., 1960, pp 469-472. ^c G. A. Jeffrey, T. H. Jordon, and R. K. McMullan, *Science*, **155**, 689 (1967).

triangles never occur, nor do any polygons whose size exceeds eight.

Molecular Dynamics Results

The polygon enumerations have been based on a set of 14 independent configurations (to which periodic boundary conditions apply) selected from a molecular dynamics run¹⁵ for water at 10° and mass density 1 g/cm³. Since the system of 216 molecules used in this simulation was relatively small, there was some initial concern that hydrogen-bond polygons of moderate size occasionally might be counted as closed when they stretch in open fashion between a molecule and its periodic image in a neighboring unit cell.¹² Therefore eight replicas of the molecular dynamics unit cell were

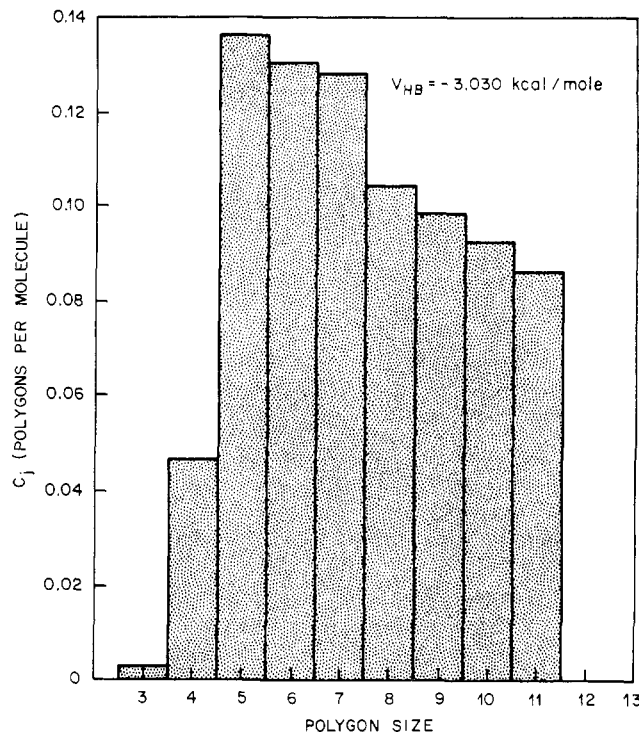


Figure 5. Polygon distribution for $V_{\text{HB(II)}} = -3.030$ kcal/mol.

arranged to form a $2 \times 2 \times 2$ larger cube, to which periodic boundary conditions again applied. The molecules were then renumbered 1 to 1728 and treated as distinguishable for the enumeration. For the polygon sizes considered, this strategy suffices to eliminate closure failures.

The computer program which accomplishes the enumeration is an adaptation of one developed by Guttman to analyze the structure of glasses.¹⁶ The procedure uses a listing, for each molecule, of the neighbors to which it is bonded. From that listing, an exhaustive branched search is constructed for bond paths which come back on themselves in three steps (triangles). Subsequently, four-bond closed paths (quadrilaterals) are sought with complete testing for short-circuiting bonds. Valid pentagons are then identified and so on to the desired degree of complexity. In the present investigation, 11-sided polygons proved to be the limit of feasibility.

Polygon counts have been carried out with four alternative values of V_{HB} , which we designate by Roman numerals.

$$\begin{aligned}
 V_{\text{HB(I)}} &= -2.121 \text{ kcal/mol} \\
 V_{\text{HB(II)}} &= -3.030 \text{ kcal/mol} \\
 V_{\text{HB(III)}} &= -3.939 \text{ kcal/mol} \\
 V_{\text{HB(IV)}} &= -4.848 \text{ kcal/mol}
 \end{aligned} \tag{6}$$

Table II collects the results, presented as C_j , the average number of non-short-circuited polygons of size j per molecule of the system. Table II also shows the average number $\langle b \rangle$ of hydrogen bonds in which a molecule simultaneously participates. Included as well are the fractions n_0 and n_1 of molecules which respectively participate in no hydrogen bonds and just one

(16) We are indebted to Dr. Lester Guttman of the Argonne National Laboratory for invaluable help in developing the program.

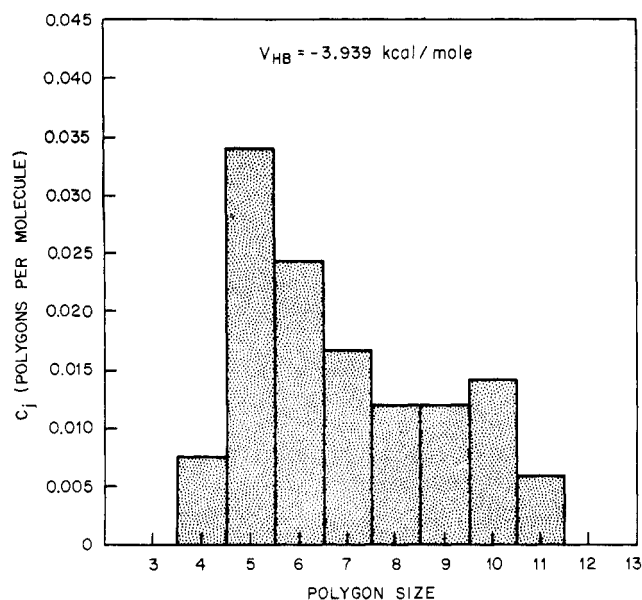


Figure 6. Polygon distribution for $V_{HB(III)} = -3.939$ kcal/mol.

Table II. Parameters Characterizing the Hydrogen-Bond Patterns in Liquid Water at 10°C and Mass Density 1 g/cm³^a

	I	II	III	IV
V_{HB} kcal/mol	-2.121	-3.030	-3.939	-4.848
$\langle b \rangle$	3.88	3.14	2.26	1.18
n_0	0	0.00331	0.0410	0.249
n_1	0.0026	0.029	0.180	0.415
C_3	0.05952	0.002976	0	0
C_4	0.1564	0.04663	0.007606	0
C_5	0.3459	0.1362	0.03406	0.001323
C_6	0.3548	0.1306	0.02447	0.0006614
C_7	0.3320	0.1280	0.01687	0
C_8	0.2715	0.1045	0.01224	0
C_9	0.1971	0.09854	0.01224	0
C_{10}	0.1118	0.09292	0.01422	0
C_{11}	0.07573	0.08664	0.005952	0

^a The mean number of hydrogen bonds terminating at a molecule is $\langle b \rangle$; n_0 is the fraction of unbonded molecules, and n_1 is the fraction with precisely one bond. C_j stands for the number of non-short-circuited polygons per molecule of the liquid, with j sides.

hydrogen bond; these classes of molecules of course can never serve as vertices of polygons. For ease of visualization the polygon concentrations have been displayed as histograms in Figures 4–7.

Discussion

Except for the case $V_{HB(IV)}$ which falls outside the range of “reasonable” hydrogen bond definitions, the polygon distributions show a significant number of polygons with sizes >8 . Although our calculations have not gone beyond size 11, it seems clear from Figures 4–6 that polygons with 12 or more sides are hardly rarities. Considering the polygon occurrences listed in Table I, it is hard to reconcile a literal view of liquid water as a recognizably disordered version of any known aqueous crystal. This conclusion is consistent with our earlier observation, based on stereoscopic pictures of molecular configurations generated during the molecular dynamics simulation, that liquid water consists

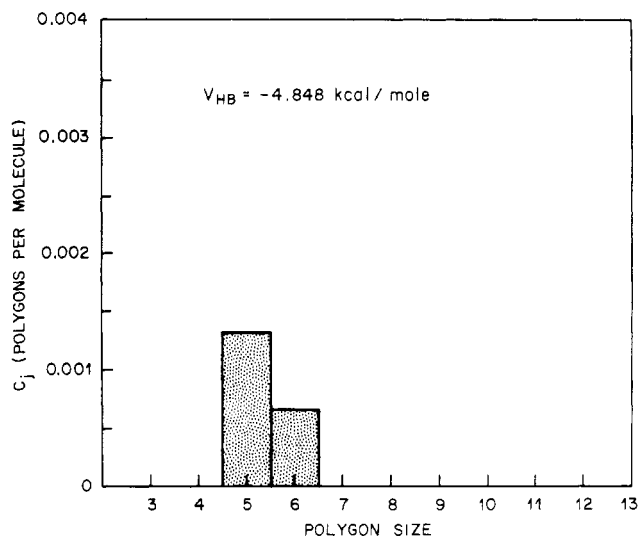


Figure 7. Polygon distribution for $V_{HB(IV)} = -4.848$ kcal/mol.

of a spatially homogeneous, random hydrogen-bond network in which no recognizable crystal patterns were visible.¹⁰

The import of Figure 7, which is based on the very stringent hydrogen bond definition IV, is that only pentagons and hexagons will exist with relatively unstrained bonds.

Case III, with results shown in Figure 6, is particularly interesting. The corresponding cutoff energy $V_{HB(III)} = -3.939$ kcal/mol agrees with the invariant point of the pair potential distribution function $p(V)$ for interaction ST2. This is the point on the negative potential energy axis for which the number of molecular pairs is independent of temperature (in the ordinary temperature regime).^{15,17} To the extent that one feels obliged to select a unique cutoff V_{HB} , this value $V_{HB(III)}$ probably qualifies strongly for consideration, since the existence of an invariant point argues for a basic hydrogen-bond rupture mechanism in the liquid.^{15,17}

The nonmonotonic behavior of the distribution shown in Figure 6, at size 10, we believe to be a real effect. With a slightly more liberal definition of the hydrogen bond (V_{HB} nearer zero) a weak short-circuiting bond would likely be identified for many of these decagons, thereby converting them to a pair of hexagons.

Our results seem to give no special support to the claim by Del Bene and Pople¹⁸ that hydrogen-bond triangles might play an important role in the structure of liquid water. Of course this might merely reflect an inadequacy of the ST2 interaction used in the present calculations. However recent accurate quantum-mechanical studies¹⁹ also do not suggest any marked stability for these water molecule trimers, though further work seems warranted.

The polygon distributions seem to show no systematic preference for even-order polygons at the expense of odd-order polygons. The lattice and cell theories mentioned in the introductory section,^{6–8} however, can only include even-order polygons as a consequence

(17) See ref 11, Figure 11, for $p(V)$ curves and their common crossing point for an interaction closely related to ST2.

(18) J. Del Bene and J. A. Pople, *J. Chem. Phys.*, **52**, 4858 (1970).

(19) B. R. Lentz and H. A. Scheraga, *J. Chem. Phys.*, **58**, 5296 (1973).

of their reliance on the body-centered cubic structure. One must therefore accept only with reservation the specific bonding patterns generated by these theories.

The major deficiencies of the molecular dynamics simulation method for water are that (a) classical statistical mechanics is utilized and that (b) the intermolecular potential has been taken to be pairwise additive. These features doubtless affect the precision of the simulation to a substantial extent, but it is difficult to argue that the qualitative conclusions which we have

reached about hydrogen-bond patterns would be significantly altered upon rectifying these deficiencies.

Obviously solutes will perturb the pattern of hydrogen bonds in water in a manner dependent on solute size, charge, shape, and chemical character. These structural shifts should be visible in the distribution of non-short-circuited polygons. It will eventually be important to see if common influences on this distribution can be verified for solutes all classed as "structure makers," or as "structure breakers."⁴

π vs. σ Structures in Imidazyl and Related Heteroradicals

E. M. Evleth,* P. M. Horowitz, and T. S. Lee

Contribution from the Centre de Mécanique Ondulatoire Appliquée, Paris, France, and The University of California, Santa Cruz, California 95064.

Received May 7, 1973

Abstract: INDO calculations on imidazyl and a number of heteroradicals indicate that there is some ambiguity as to their predicted ground state symmetries. Experimentally, only a few examples of the esr spectra of these types of radicals are known. Sufficient data exists, however, to allow one to predict that the results obtained from INDO predictions are not necessarily computational artifacts. π -electron SCF single annihilation calculations of the electronic structures of pyrrolyl, imidazyl, and other related structures were also carried out. Here, too, there is some doubt as to the reliability of the results. In some cases small parameter changes yield significantly different computed spin and electron densities. Simple resonance structure arguments are imposed to rationalize the spin density variations in the π -electron calculations. Finally, a state symmetry analysis is proposed which predicts that the potential energy surfaces of ground and excited states of some even and odd electron structures cross at some coordinates involving the stretch of C-H or N-H bonds.

This paper addresses itself to three main topics. First we will explore the intuitive ambiguities of attempting to assign the ground state symmetries of a number of heteroradicals. We will also explore the difficulty of obtaining "good" π -electron spin density calculations. Finally we will also explore the state symmetry consequences of these assignments with respect to the photogeneration of such radicals from parent filled shell molecules.

Conceptual ambiguities exist with respect to intuitively assigning the symmetry of the ground state of planar radicals. Kasai and coworkers¹ set out to explore this issue with respect to the ground state symmetries of the phenyl and higher polycyclic aromatic radicals. Kasai showed¹ that in the systems studied aryl radicals invariably had σ structures. The simplest resonance structure representation of the σ -phenyl radical is as shown below. The π radical is an excited state of the phenyl radical. At this time we will avoid the problem of assigning the proper group theoretical representations for various resonance structures. This would require writing a number of additional structures of proper phasing. In our diagrams we use the Salem-Dauben-Turro convention² of circling the σ electrons and giving the summation of the total number of π and σ electrons involved in the critical portion of the bonding picture.



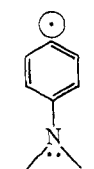
$6\pi, 1\sigma$



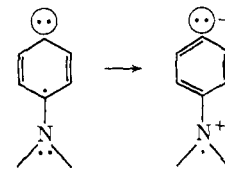
$5\pi, 2\sigma$

single structure representations of the ground and excited state of the phenyl radical

Kasai's experimental results were also supported by INDO calculations. Kasai specifically explored the possibility that in electron-rich systems the π orbitals might yield up an electron to a half-filled σ orbital to generate a π radical. In the case of a substituted phenyl radical the electron-donating substituent might stabilize the normally energetically unfavorable zwitterionic resonance structure to yield such a π radical, as shown below. INDO calculations,³ however, in-



$8\pi, 1\sigma$
 σ radical



$7\pi, 2\sigma$
 π radical

structure representations of the σ and π *p*-aminophenyl radicals

(1) P. H. Kasai, E. Hedaya, and E. B. Whipple, *J. Amer. Chem. Soc.*, **91**, 4364 (1969); P. H. Kasai, *Accounts Chem. Res.*, **4**, 329 (1971).

(2) L. Salem, W. G. Dauben, and N. J. Turro, *J. Chim. Phys.*, **70**, 649 (1973).

(3) E. M. Evleth and P. M. Horowitz, *J. Amer. Chem. Soc.*, **93**, 5636 (1971). The symmetry of the *p*-aminophenyl cation is predicted to be 3B_1 not 3A_1 as stated in Table II of this reference.